Draft version May 2, 2007
Preprint typeset using LaTeX style emulateapj v. 11/12/01

AN UNUSUAL CIRCUMSTELLAR DEBRIS STRUCTURE ASSOCIATED WITH THE NEARBY, SUN-LIKE STAR HD 61005

Dean C. Hines[1], Glenn Schneider[2], Eric E. Mamajek[3], Stanimir A. Metchev[4], Hollenbach, David[5], Lynne A. Hillenbrand[6], Michael R. Meyer[2], Dana K. Backman[7], Jeroen Bouwman[8], John M. Carpenter[6], Thomas Henning[8], Jinyoung Serena Kim[2], Amaya Moro-Martín[9], Joan Najita[10], Murray D. Silverstone[11], Jens Rodmann[8], Sebastian Wolf[8]

Draft version May 2, 2007

ABSTRACT

We present the discovery of an unusual circumstellar structure associated with the 100±50 Myr old, nearby (34.6±1.1 pc), sun-like G-dwarf star HD 61005. *Spitzer* IRAC, IRS & MIPS observations, conducted as part of the FEPS *Spitzer* legacy science survey of sun-like stars, detail the nature of thermal emission from the object that is in excess of the expected stellar photosphere. Follow-up 0.″1 spatial resolution *HST*/NICMOS 1.1 μm coronagraphic images reveal a very bright structure (flux density $\sim 18 \pm 3.3$ mJy, $0.77\% \pm 0.16\%$ that of the $J_{mag} = 6.91$ star) that scatters starlight to distances as far as 7″ ($\sim$ 240 AU) from the occulted star. The structure exhibits a strong asymmetry about its morphological major axis, but is mirror-symmetric about its minor axis (envision a wing-spread moth with the star as the head). The scattered light is traced inward to within 10 AU of the star (limited by the coronagraphic obscuration) with no evidence of a turnover in radial surface brightness profiles. The fraction of 1.1 μm starlight scattered by the structure at $r > 0.''3$ is larger than any debris disk previously observed, and exceeds that of β Pictoris by more than a factor of 2. This extremely high scattered fraction compared with $L_{IR}/L_* \approx 2 \times 10^{-3}$ suggests that the scattering particles are small ($a \sim 1.1\mu m/2\pi \sim 0.2\mu m$), much smaller than the blowout size ($a \approx 0.3\mu m$). The extraordinary, swept morphology of material may be explained by the motion of the HD 61005 system through its local interstellar medium.

Subject headings: circumstellar matter — infrared: stars — planetary systems: protoplanetary disks — stars: individual (HD 61005)

1. INTRODUCTION

Our knowledge of the formation and evolution of planetary systems has evolved rapidly within the last two decades. The landmark discovery made with *IRAS* of excess IR emission associated with the A-star Vega (Aumann et al. 1984) proved conclusively that circumstellar material analogous to the debris found in our solar system can exist around another main sequence star. Subsequent *IRAS* and *ISO* detections of stars with IR excesses (e.g., Mannings & Barlow 1998; Spangler et al. 2001)[12] showed that debris, presumably arising from colliding planetasimals, is fairly common (e.g., Lagrange et al. 2000; Meyer et al. 2007, and references therein).

The *Spitzer* Space Telescope Legacy Science program entitled the Formation and Evolution of Planetary Systems (FEPS) was designed to extend the earlier *IRAS* and *ISO* results to sun-like stars of spectral types F8V through K3V and ages from 3 Myr to 3 Gyr (Meyer et al. 2004; 2006). The FEPS survey has now successfully identified many new candidate debris systems with infrared emission in excess of that expected from the stellar photosphere (Meyer et al. 2004; Kim et al. 2005; Hines et al. 2006; Moro-Martín et al. 2007; Hillenbrand et al. 2007; Carpenter et al. 2007).

Models of the spectral energy distributions (SEDs) of these newly identified debris systems place constraints on the temperature and size distribution of the material, but cannot uniquely determine the spatial distribution; the objects are unresolved by *Spitzer*. Single-dish sub-mm observations are limited to spatial resolutions of 10-20″, and sub-mm interferometry is so far limited to a few arcseconds, comparable with *Spitzer*. Currently, only high spatial resolution (sub-arcsecond) images of scattered light can address questions such as: 1) the exact radial extent of the material; 2) the grain surface density distribution; and 3) whether the disk exhibits azimuthal asymmetries indicative of particle shepherding by unseen planets.

[1] Space Science Institute, 4750 Walnut Street, Suite 205 Boulder, CO 80301.
[2] Steward Observatory, The University of Arizona, 933 N. Cherry Ave., Tucson, AZ 85721.
[3] Harvard-Smithsonian Center for Astrophysics, 60 Garden Street, Cambridge, MA 02138.
[4] University of California, Los Angeles, CA.
[5] NASA Ames, Moffet Field, CA 04035.
[6] Astronomy, California Institute of Technology, Pasadena, CA 91125.
[7] SOFIA, Mail Stop 211-3, NASA-Ames, Moffet Field, CA 94035-1000.
[8] Max-Planck-Institut fur Astronomie, Konigstuhl 17, D-69117 Heidelberg, Germany.
[9] Department of Astrophysical Sciences, Princeton University, Princeton, NJ 0854.
[10] National Optical Astronomy Observatories, AURA
[11] Eureka Scientific, 10813 Graeloch Road, Laurel, MD 20723-1124.
[12] The sensitivity of both missions limited discovery primarily to fairly luminous, A & F, dwarf stars and younger pre-main-sequence stars.

Therefore, we have begun extensive follow-up observations of FEPS-identified debris systems using the *HST*/NICMOS (near-IR) coronagraph to look for, spatially map, and obtain surface brightness measurements of starlight-scattering, circumstellar material. Here we report images of 1.1μm light scattered by material in the close circumstellar environment of the 50-150 Myr old, late G dwarf star, HD 61005 [HIP 36948, SAO 198166; d = 34.6 ± 1.1 pc (Perryman 1997)]. The remarkable structure revealed by these observations is unlike any other debris systems observed previously.

2. OBSERVATIONS

HD 61005 was observed in the FEPS survey (PID 148) with all three science instruments on the *Spizter* Space Telescope (Werner et al. 2004) using the procedures described in detail by Meyer et al. (2006). Reduction of the data followed the detailed procedures used for the entire FEPS survey (Carpenter et al. 2007) as generally outlined in previously FEPS contributions (Kim et al. 2005; Hines et al. 2006; Bouwman et al. 2007).

IRAC and MIPS[13] photometry for HD 61005 are presented in Table 1, along with synthetic photometry at 13, 24 and 33 μm derived from a low (spectral) resolution IRS spectrum using rectangular FWHM band-passes of 1.6, 4.7 and 5 μm, respectively. These IRS flux densities are the error–weighted means within each passband. Table 1 also includes a 60 μm detection from *IRAS* (HD 61005 was not detected in the other three *IRAS* bands).

HD 61005 was observed with the coronagraph in NICMOS camera 2 (scale: 75.8 mas pixel^{-1}) using the F110W (λ_{eff} = 1.104 μm, FWHM = 0.5914 μm) filter. Coronagrahic images were obtained at two celestial orientations differing by 131 degrees in the frame of the camera 2 detector. Such observations enable post-processing discrimination against, and reject of, rotationally invariant optical artifacts in imperfect PSF subtracted images (notably residuals from the HST diffraction spikes, but other artifacts as well). The observing strategy, data calibration methodology and reduction techniques follow those outlined in Schneider, Silverstone & Hines 2005 (SSH05) used successfully in HST GO program 10177 (PI: Schneider). Details of the HD 61005 observing plan are captured in the publicly available Phase II definition of the GO 10527 program[14].

Instrumentally calibrated count rate images were created from the individual F110W coronagraphic multiaccum frames. For each target/visit (orientation) the individual images were median combined after verifying the repeatability of the intra-visit images within the typical range of inter-image stability. Well characterized instrumentally induced artifacts associated with the detector/readout electronics were removed following the procedures in SSH05, This step was perfomed on all targets in the GO 10527 program including those of the PSF template observations later applied to the HD 61005 observations.

All similarly processed and instrumentally calibrated count rate images obtained from the GO 10527 program that showed no evidence of scattered light excesses themselves were tested for suitability as PSF templates. The efficacy of PSF subtractions requires target/template PSFs to (*a*) be well matched in J-H color index (usually |J-H |≤ 0.3), (*b*) have roughly comparable "breathing" phase space (relative *HST* secondary mirror despace excursions $\lesssim 1\mu$m; as empirically determined from residual PSF structure), and (*c*) have close repeatability of the NICMOS camera 2 cold mask position (which has small thermally driven metrologic instabilities). For the first orientation HD 61005 observation (denoted "Visit 16") ten suitable template PSFs were found from the GO 10527 target set, and five for the second orientation (Visit 15) observation. All images were co-registered in detector coordinates about the location of HD 61005 image in the Visit 16 image, and corrected for the $\sim 0.7\%$ linear geometrical distortion in Camera 2. All images were flux scaled (initially) to an F110W magnitude of 5.0 based upon 2MASS catalog photometry transformed from J-band using the *calcphot* task in the STSDAS package. In doing so we assumed the stellar spectral type G8V (§4). The F110W transformed magnitudes were cross-checked as described in SSH05 using "TinyTim" model PSFs matched in intensity to wings of short, but core-saturated, contemporaneously obtained non-coronagraphic images of the stars. The individual images comprising the two sets of PSF templates (one set of ten and one set of five) were subtracted from their paired HD 61005 observations, resulting in fifteen PSF-subtracted images of HD 61005.

Artifact (diffraction spike and other low-spatial frequency mismatched PSF subtraction residuals) rejection masks were individually made for the full set of PSF subtracted images. The two sets of HD 61005 PSF-subtracted masked images from each orientation were, separately, median combined (rejecting pixels for each image based upon the masks before median combination). This resulted in two artifact-rejected median-combined PSF-subtracted images (one for each HD 61005 visit). These two images were then both rotated to a "north up" orientation, and combined, but rejecting pixels unsampled (e.g. along diffraction spikes or other individually commonly masked masked artifacts) in either image.

As a check on the procedure, the two images were combined in two ways: first by a simple (masked) mean for the two visits; and second by a weighted mean of the two visits, with 2:1 weights for visits 16 & 15 predicated upon the number of input images after pixel masking. The resulting images (as expected) differ slightly, but these differences speak to the dispersion in the detailed structure of the input images. The "final" image which we speak to in the remainder of the paper is based upon the weighted mean combination.

To verify that the fidelity of the circumstellar scattered-light structure seen in the HD 61005 image, we followed the same process multiple times but choosing (each time) a different image from the PSF template set as a (null) test target in place of HD 61005. All of the resulting "PSF-minus-PSF" images showed no features bearing any resemblance to circumstellar scattered-light seen in the HD 61005 processed images. The dispersion in the (much lower level) remaining instrumentally diffracted and scattered light in

[13] The FEPS survey did not obtain MIPS 160 μm observations for this object.

[14] http://www.stsci.edu/observing/phase2-public/10527.pdf

the PSF-minus-PSF images was used to assess the systematic uncertainties in the flux density measures in the HD 61005 processed images.

3. THERMAL EMISSION AND SCATTERED LIGHT

Figure 1 shows the SED of HD 61005. For completeness we show the *IRAS* 12, 25 & 100 μm upper limits, a *IRAS* 60 μm detection, and a 1.2 mm upper limit (Carpenter et al. 2005). The SED is well fit by a Kurucz model ($T_{\rm eff}$ = 5456 K) from the optical through $\approx 8\mu$m, but shows a strong excess for $\lambda > 18\mu$m. The IRS spectrum (inset in Fig. 1) is not dominated by obvious spectral features, implying that the thermal emission does not originate from hot, small grains that would produce strong silicate emission features. Figure 1 also shows a T = 60K blackbody SED, scaled to the 24, 60 and 70 μm photometry, that yields $L_{\rm IR}/L_* \approx 2 \times 10^{-3}$. This blackbody temperature provides a minimum distance of the material of $\gtrsim$ 16 AU, using $L_*/L_\odot = 0.55$ (from integrating the best fit Kurucz model). Additional modeling as part of an ensemble study of FEPS-identified, cool debris disks, suggests that the SED may be better fit by an extended ($7 \lesssim R_{\rm dust} \lesssim 70$ AU disk, with a $\sim \pm$10K dispersion in black body temperatures around 60K (Hillenbrand et al. 2007). Grains that radiate efficiently at $\sim 70\mu$m, and are in radiative equilibrium with the stellar radiation field will have $a \gtrsim \lambda/2\pi \sim 10\mu$m, but we cannot rule out smaller grains that radiate less efficiently, and would thus be farther from the star (see, e.g., Fig. 5, Hines et al. 2006).

Figure 2 shows the 1.1 μm scattered light image as a $\log_{10}$ color-coded contour map, with the corresponding image inset. The grey circle at image center represents the 0.″3 radius coronagraphic obscuration (corresponding to r = 10.3 AU at the 34.6pc distance of HD 61005). The pattern of scattered light (resembling a Moth) is asymmetric about its morphological major axis and mirror-symmetric about its minor axis. The scattered starlight extends to $\sim$ 3″ (105 AU) along the minor axis to the southeast (celestial PA = 160 deg) and $\sim$6″ (210 AU) both sides of the star along the "major axis." The maximum extent of the scattered light pattern (the "wingtips of the Moth" below the major, and toward the minor, axis) is $\sim$ 7″(242 AU). Very little scattered starlight is detected in the northwest sector flanking the minor axis. At $r = 0.75''$, the on-axis ratio of the south-east to north-west scattered light is $\sim$ 12, and at 2 ″ NW, there is no scattered light detected above the residual background noise. The total 1.1μm flux density within an annulus from $0.''3 \leq r \leq 5''$ is F(F110W) = 18 mJy $\pm$ 3.3 mJy. This yields a 1.1μm scattering fraction $f_{\rm disk}/f_* = 0.77\% \pm 0.16\%$. This overall morphology is verified in optical coronagraphic images obtained with HST/ACS (S. Metchev, private comm).

Figure 3 presents radial surface brightness profiles for three crosscuts; one along the southern semi-minor axis, and two along the peak surface brightness ridges extending "below" the major axis on either side of the star. While we measure positive flux densities very close to the occulting edge of the coronagraphic hole, we conservatively show only the profiles for $r \geq 0.''7$ where we are confident that systematics do not dominate the result. The surface brightness profiles from $0.''7 \leq r \leq 5.''0$ along both sides of the star in the direction of the ridge of maximum brightness at $r = 5''$ are well represented by unbroken $r^{-2.5}$ and $r^{-2.7}$ power law fits for the east and west extensions, respectively. Beyond 0.″7, the surface brightness profile along the southern semi-minor axis is well fit by broken $r^{-2.0}$ and $r^{-5.0}$ power laws, for $0.''7 \leq r \leq 1.''4$, and $1.''4 \leq r \leq 2.''6$, respectively; shallower interior, and steeper exterior, to the break at $r = 1.''4$ than the profiles along the ridges of maximum brightness in the "wings of the Moth".

4. THE EVOLUTIONARY STATUS OF HD 61005

HD 61005 is reported as G3/5V in Houk et al. (1982), but Nordstrom et al. (2004) infer $T_{\rm eff}$ = 5346K from the Stromgren indecies, suggesting a $\sim$ G9.5 spectral type. Based on published photometric colors, we find that the spectrum is well fit by a Kurucz model with $T_{\rm eff}$ = 5456 K, consistent with a G8V spectral type (Fig. 1), which agrees well with the G8Vk listed by Gray et al. (2006).

Observations of CaII ($\log R'_{\rm HK}$ = -4.30: Soderblom et al. in prep; Gray et al. 2006; Henry et al. 1996), Hα emission (EW(Hα) = 136$\pm$6 m$\AA$: Waite et al. 2005) and soft X-ray emission ($\log L_{\rm X}$ = 29.2: Wichmann, Schmitt & Hubrig 2003) show that HD 61005 is chromospherically active, but not actively accreting. The star does not show optical variability over a two year timescale ($\Delta V \leq$ 0.01mag: Menzies, Marang, & Westerhuys 1990).

The UVW heliocentric velocity vector of HD 61005 (-22.9, -14.0, -4.1 km s^{-1}) $\pm$ (0.4, 0.4, 0.3 km s^{-1}) is well-constrained, and its very negative U-velocity component places the star away from the velocity locus for most $<$ 100 Myr-old stars within 100 pc (see e.g. Asian et al. 1999; Chen et al. 1997). Except for stars of type B5 and later, there are no B stars within 100pc of the Sun that have motions similar to HD 61005; this at least suggests that the motion of HD 61005 would be somewhat unusual compared to that of stars with ages of $<$ 80 Myr within 100 pc of the Sun. Interestingly, though, its UVW vector is almost exactly coincident (within 2 km/s) with the $\sim$ 50-Myr-old $\sim$ 150-pc-distant IC 2391 open cluster (-22.9, -13.6, -6.0)($\pm$ 0.8, 0.3, 0.2) (Robichon et al. 1999). To appreciate how close this is, out of 13239 stars in the Nordstrom et al. (2004) catalog with UVW vectors, only 3 (0.02%) have UVW space motions closer to IC 2391 than HD 61005. Investigation of any possible kinematic link between HD 61005 and IC 2391 is beyond the focus of this study, but if the star is an outlier of IC 2391 (or any unbound, now-dispersed associations that formed contemporaneously with the IC 2391 cluster), then this would point toward an age of $\sim$50 Myr (Barrado y Navascués, Stauffer, & Jayawardhana 2004).

The CaII H&K emission suggests $t_{\rm star} \sim$ 135 Myr (Mamajek & Hillenbrand, in prep.), and the lithium absorption (EW(Li) = 164 m$\AA$: Wichmann, Schmitt & Hubrig 2003) implies $t_{\rm star} \sim$ 50 Myr upon comparison to Li values for late G stars in young clusters of known age. Given these indicators and the space motion, we estimate the age to be 100$\pm$50 Myr[15].

5. THE CIRCUMSTELLAR MATERIAL ASSOCIATED WITH HD 61005

[15] $M/M_\odot$ = 0.84 (Nordstrom et al. 2004), but the $\sim$ZAMS mass is $M/M_\odot$ = 0.95 (Mamajek, in prep).

Although the near-IR scattered light image is remarkably similar to that observed for the classical T-Tauri star GM Aur (Schneider et al. 2003), the SED, including the lack of active accretion signatures and infrared excess at $\lambda \lesssim 8\mu$m, argues against a T-Tauri-like disk. Furthermore, optically thick disks around pre-main-sequence stars such as TW Hydrae (de la Reza et al. 1989; Weinberger et al. 2000) and Hen 3-600 (de la Reza et al. 1989; Low et al. 2006) in the $t_{\rm star} \sim 8$ Myr old TW Hydra Association (TWA: Webb et al. 1999) both show thermal emission over a large range of temperatures, with large Lir/Lstar (e.g., Low et al. 2006). The estimated age of HD 61005 ($t_{\rm star} \sim 80 - 150$ My) also argues against this interpretation, since the oldest T-Tauri objects are $\sim 15 - 25$ Myr (Mamajek et al. 2002, White & Hillenbrand 2004). If HD 61005 posed an optically thick disk, it would be the oldest example known by at least a factor of two in age.

The unique morphology of HD 61005 could result from the star illuminating a cloud within the interstellar medium, as was shown for the (Kalas et al. 2002). However, unlike those examples, HD 61005 is well within the "local bubble," and there is no evidence of extended interstellar structure in the the MIPS 24 and 70μm images; the images of HD 61005 are unresolved by *Spitzer*. Instead, we suggest that the material is physically associated with HD 61005, and is debris resulting from the erosion/collision of planetesimals orbiting the star.

An important clue to the origin of the shape of the scattering structure comes from the space motion, which is 12 km s^{-1} relative to the local ISM and points approximately NNW in Figure 2 (the "direction" of flight of the moth). Thus the swept morphology could result from ram pressure on small grains in the outer regions of the debris disk. Such a mechanism has been discussed (Lissauer & Griffith 1989) and considered as a warping mechanism for βPic (Artymowicz & Clampin 1997) and HD 32297 (Kalas 2005).

The balance between ram pressure and gravitational force in the vertical direction (relative to the disk plane) can be expressed as a function of the vertical displacement fraction

$$\frac{z}{r} = f \sim 10^{-4} \left(\frac{n}{cm^3}\right) \left(\frac{r}{100AU}\right)^2 \left(\frac{1um}{a}\right) \left(\frac{v}{10km/s}\right)^2.$$

From Figure 2, the warp begins to strongly manifest for $r \gtrsim 100$AU, and $f \sim 0.3$. This yields a ratio of ISM density to ram stripped particle size of $\sim 3 \times 10^3$. The local bubble is nearly void of diffuse clouds (Franco 1990), limiting the densities to ~ 100cm^{-3}. This would imply that the dust we see in the swept wings of the moth would be quite small $a \lesssim 0.1\mu$m. Such grains are much smaller than the blowout size ($a_{\rm blowout} \sim 0.3\mu$m, so would not survive long within the system.

The timescale for grain migration due to PR-drag is about one thousand times longer than the collision time; the evolution of material around HD 61005 is dominated by collisions, and the loss of material from the system is dominated by grain blow out. The blowout time for grains launched between 16 and 100AU is $\sim 30 - 500$ yrs, similar to the orbital time scales at these distance. A recent dust production event within the disk could have produced the small particles that we see in the outer regions of the disk.

Alternatively, the small particles could be Bondi-accreted ISM particles (e.g., Lissauer & Griffith 1989). The accreted material forms an orbiting disk of interstellar gas and dust at a radius that is smaller than, but assumed comparable to, the Bondi radius, which is ~ 10AU for the velocity of ~ 10 km s^{-1} for HD 61005. The gas then accretes onto the star via MRI instability, with $\alpha = 0.01$; the dust blows out via radiation pressure.

Such small grains would also explain the large 1.1μm scattered light fraction compared with the fractional dust luminosity; the grains we see in scattered light are extremely efficient scatterers, but do not contribute significantly to the thermal excess. Grains $a \sim 1.1\mu{\rm m}/2\pi \sim 0.2\mu$m would satisfy this constraint, and would also be readily expelled from the system. Very small grains may also explain the powerlaw break in the surface brightness distribution along the minor axis (Fig. 3); forward superimposed on back-scattering. A full exploration of the thermal and scattering properties of the system will be presented in a future contribution that will also present optical and near-IR polarimetry obtained with the HST/ACS and HST/NICMOS (Metchev et al., in prep).

6. CONCLUSION

We have discovered a very unusual circumstellar structure associated with the 100±50 Myr old, sun-like star HD 61005. In particular:

- The thermal SED and the age of the system suggest that the material is associated with debris rather than remnants of the primordial disk.
- The structure seen in scattered 1.1μm light is highly asymmetric, rather than the more symmetric debris disks and rings seen in other stars of similar age with thermal infrared excesses.
- The fraction of 1.1μm starlight scattered by the structure at r > 0.″3 is larger than any debris disk previously observed, and exceeds that of β Pictoris by more than a factor of 2.

The swept shape of the debris disk may be caused by the motion of the HD 61005 system through its local interstellar medium. New data such as planned, *HST* multi-wavelength coronagraphic polarimetry, together with more *Spitzer* (and future Herschel) data will further elucidate the nature of this object.

This investigation was based [in part] on observations made with the NASA/ESA Hubble Space Telescope, obtained at the Space Telescope Science Institute (STScI), which is operated by the Association of Universities for Research in Astronomy, Inc., under NASA contract NAS 5-26555. These observations are associated with program GO10527, support for which was provided by NASA through a grant from STScI. This work is also based [in part] on observations made with the Spitzer Space Telescope, which is operated by the Jet Propulsion Laboratory, California Institute of Technology under NASA contract 1407. FEPS is pleased to acknowledge support from NASA contracts 1224768 and 1224566 administered through JPL. This publication makes use of data products from the Two

Micron All Sky Survey, which is a joint project of the University of Massachusetts and the Infrared Processing and Analysis Center/California Institute of Technology, funded by the National Aeronautics and Space Administration and the National Science Foundation. We have also made use of the SIMBAD database.

REFERENCES

Asian et al 1999, A&A 341, 427

Artymowicz, P. & Clampin, M. 1997, ApJ, 490, 863

Aumann, H. H., et al. 1984, ApJ, 278, L23

Barrado y Navascués, D., Stauffer, J. R., & Jayawardhana, R. 2004, ApJ, 614, 386

Bouwman, J. et al. 2007, ApJ, submitted

Butler, R. P., et al. 2006, ApJ, 646, 505

Cannon, A. J., & Pickering, E. C. 1993, VizieR Online Data Catalog, 3135, 0

Carpenter, J. M., Wolf, S., Schreyer, K., Launhardt, R., & Henning, T. 2005, AJ, 129, 1049

Carpenter, J. M. et al. 2007a, in prep

Carpenter, J. M. et al. 2007b, in prep

Chen et al. 1997 A&A 318,29

de la Reza, R., Torres, C. A. O., Quast, G., Castilho, B. V., & Vieira, G. L. 1989, ApJ, 343, L61

Franco, G. A. P. 1990, A&A, 227, 499

Gray, R. O., Corbally, C. J., Garrison, R. F., McFadden, M. T., Bubar, E. J., McGahee, C. E., O'Donoghue, A. A., & Knox, E. R. 2006, AJ, 132, 161

Henry, T. J., Soderblom, D. R., Donahue, R. A., & Baliunas, S. L. 1996, AJ, 111, 439

Hillenbrand, L.A. et al. 2007, ApJ, in prep

Hines, D. C., et al. 2006, ApJ, 638, 1070

Houk, N. 1988, Michigan Catalogue of Two-dimensional Spectral Types for the HD Stars (Ann Arbor : Univ. Michigan; distributed by University Microfilms International)

Kalas, P., Graham, J. R., Beckwith, S. V. W., Jewitt, D. C., & Lloyd, J. P. 2002, ApJ, 567, 999

Kalas, P. 2005, ApJ, 635, L169

Kalas, P., Graham, J. R., Clampin, M. C., & Fitzgerald, M. P. 2006, ApJ, 637, L57

Kim, J. S., et al. 2005, ApJ, 632, 659

Lagrange, A.-M., Backman, D. E., & Artymowicz, P. 2000, Protostars and Planets IV, 639

Lissauer, J. J., & Griffith, C. A. 1989, ApJ, 340, 468

Low, F. J., Smith, P. S., Werner, M., Chen, C., Krause, V., Jura, M., & Hines, D. C. 2005, ApJ, 631, 1170

Mamajek, E. E., Meyer, M. R., & Liebert, J. 2002, AJ, 124, 1670

Mannings, V., & Barlow, M. J. 1998, ApJ, 497, 33

Marcy, G. & Butler, P. 1998, ARAA, 36, 57

Mason, B. D., Henry, T. J., Hartkopf, W. I., Ten Brummelaar, T., & Soderblom, D. R. 1998, AJ, 116, 2975

Menzies, J. W., Marang, F., & Westerhuys, J. E. 1990, South African Astronomical Observatory Circular, 14, 33

Meyer, M. R., & Beckwith, S. V. W. 2000, LNP Vol. 548: ISO Survey of a Dusty Universe, 548, 341

Meyer, M. R., et al. 2004, ApJS, 154, 422

Meyer, M. R., et al. 2006, PASP, 118, 1690

Meyer, M. R., Backman, D. E., Weinberger, A. J., & Wyatt, M. C. 2007, Protostars and Planets V, 573

Moro-Martín, A., et al. 2007, ApJ, 658, 1312

Nordström, B., et al. 2004, A&A, 418, 989

Perryman, M. A. C. & ESA 1997, The Hipparcos and Tycho catalogues. ESA SP Series Vol. 1200

Robichon, N., Arenou, F., Mermilliod, J.-C., & Turon, C. 1999, A&A, 345, 471

Rocha-Pinto, H. J., & Maciel, W. J. 1998, MNRAS, 298, 332

Schneider, G., et al. 1999, ApJ, 513, L127

Schneider, G., Silverstone, M. D., & Hines, D. C. 2005, ApJ, 629, L117

Schneider, G., et al. 2006, ApJ, 650, 414

Smith, P. S., Hines, D. C., Low, F. J., Gehrz, R. D., Polomski, E. F., & Woodward, C. E. 2006, ApJ, 644, L125

Soderblom, D. R., Henry, T. J., Shetrone, M. D., Jones, B. F., & Saar, S. H. 1996, ApJ, 460, 984

Soderblom, D. R., et al. 1998, ApJ, 498, 385

Soderblom, D. R., King, J. R., Hanson, R. B., Jones, B. F., Fischer, D., Stauffer, J. R., & Pinsonneault, M. H. 1998, ApJ, 504, 192

Spangler, C., Sargent, A. I., Silverstone,M. D., Becklin, E. E., & Zuckerman, B. 2001, ApJ, 555, 932

Waite, I. A., Carter, B. D., Marsden, S. C., & Mengel, M. W. 2005, Publications of the Astronomical Society of Australia, 22, 29

Weinberger, A. J., et al. 2002, ApJ, 566, 409

Werner, M. W., et al. 2004, ApJS, 154, 1

Webb, R. A., Zuckerman, B., Platais, I., Patience, J., White, R. J., Schwartz, M. J., & McCarthy, C. 1999, ApJ, 512, L63

White, R.J.. & Hillenbrand, L.A. 2004

White, R.J., Gabor, J. & Hillenbrand, L.A. 2006, ApJ, in press

Wichmann, R., Schmitt, J. H. M. M., & Hubrig, S. 2003, A&A, 399, 983

TABLE 1
Spitzer & *IRAS* PHOTOMETRY OF HD 61005

Band	Wavelength (μm)	Flux Density (mJy)	$\sigma_{\rm int}$ (mJy)	$\sigma_{\rm tot}$[a] (mJy)	Instrument
3.6	3.535[b]	755.06	...	16.21	*Spitzer*/IRAC
4.5	4.502[b]	463.90	...	10.65	*Spitzer*/IRAC
8.0	7.735[b]	172.45	...	3.68	*Spitzer*/IRAC
13[d]	13.17	62.34	...	3.08	*Spitzer*/IRS
24	23.68[b]	41.49	...	1.70	*Spitzer*/MIPS
24[c,d]	...	45.53	...	2.80	*Spitzer*/IRS
33[c]	...	109.98	...	6.74	*Spitzer*/IRS
60[e]	60	446.5	28.3	28.3	*IRAS*
70	71.42[b]	628.7	...	45.4	*Spitzer*/MIPS

[a]The total uncertainty ($\sigma_{\rm tot}$) is the *rss* of the "internal" measurement uncertainty (precision) and the "calibration" uncertainties (accuracy).

[b]Weighted average wavelengths.

[c]Synthetic band-pass photometry with 1.6, 4.7 and 5μm band-widths (FWHM) for 13, 24 and 33μm respectively.

[d]The MIPS 24μm photometry has not had a color-correction applied. The current value for the color-correction would yield $F_c = 1.014 \times F_{\rm obs} = 42.1$ mJy).

[e]A color correction $F_c = 0.717 \times F_{\rm obs}$ has been applied as per ***

References. — WE MAY NOT INCLUDE TABLE. IF SO, NEED TO ADD INTERNAL ERROR AND FIX SIG DIGITS. SHALL WE ADD THE SUB-MM AND THE MIPS 160?

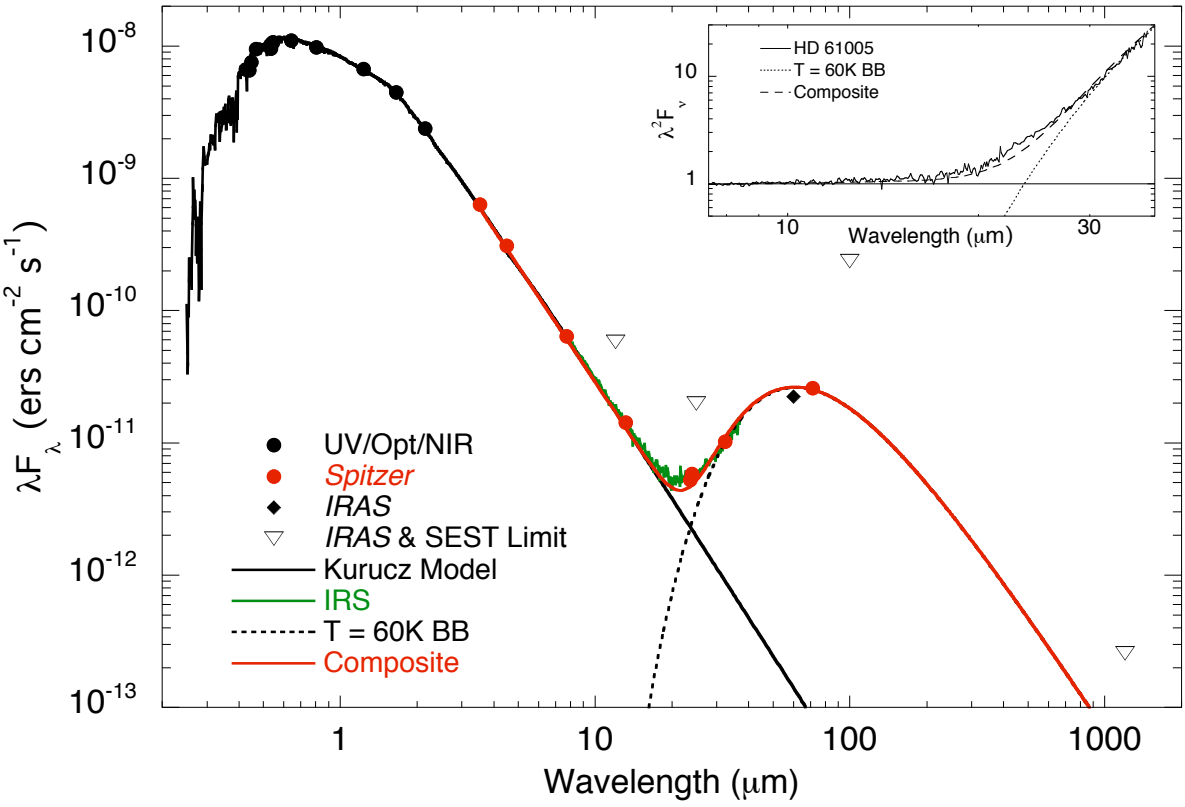

FIG. 1.— The spectral energy distribution of HD 61005 showing the Kurucz model that best fits the optical and near-IR photometry (solid curve), the ground and space-based photometry (solid symbols) and the IRS spectrum (green curve). The 1σ error bars for each point are smaller than the symbol sizes. We also show upper limits at 12, 25 and 100μm from *IRAS*, and at 1.23mm from SEST (Carpenter et al. 2005). The T = 60K blackbody fits the 24 and 70μm photometry. The inset shows the observed IRS spectrum multiplied by λ^2 and normalized at 7.5μm. The spectrum clearly deviates from Rayleigh-Jeans for $\lambda \geq 18\mu$m.

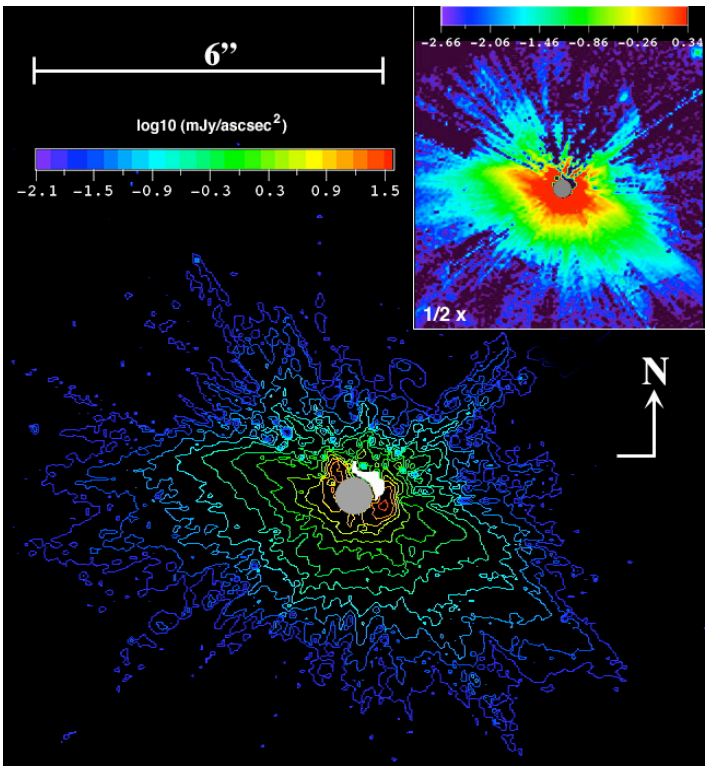

FIG. 2.— 1.1 μm $\log_{10}$ isophotal contour map of the circumstellar region about HD 61005 derived from the two-orientation combined PSF-subtracted coronagraphic image (image inset at half spatial scale). Surface brightness contour intervals are shown every [0.3] dex from 7.9 μJy arcsec^{-2} to 31.6 mJy arcsec^{-2}, and the Log_{10} image inset shows a stretch from 2.18 μJy arcsec^{-2} to 2.18 mJy arcsec^{-2}. The central grey circle represents the $r = 0\farcs3$ *HST*/NICMOS coronagraphic obscuration. The small region immediately adjacent to the obscuration to the NW (masked white in contour map, black in image) is invalid due to residual image artifacts at that location.

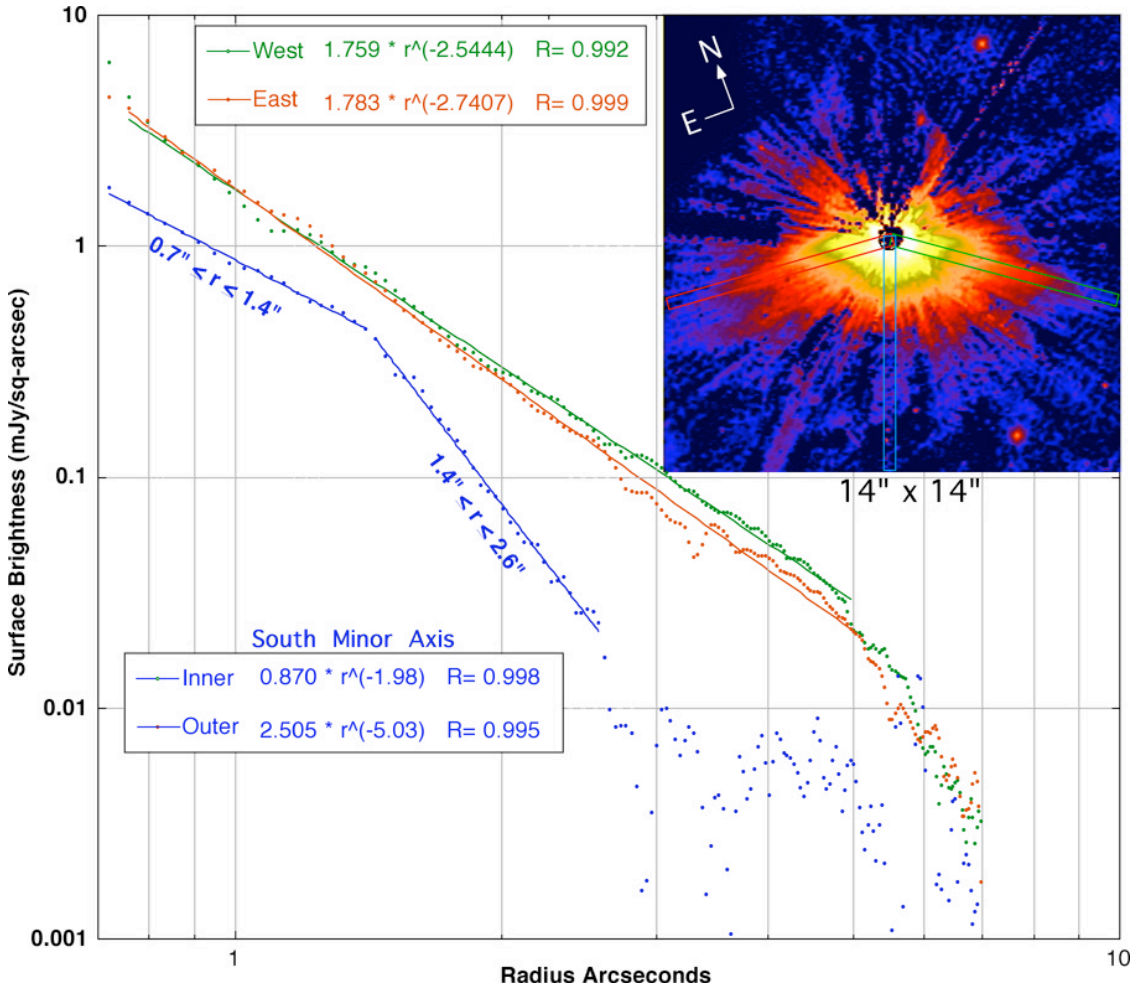

FIG. 3.— The radial decline in the scattered starlight surface brightness (measured in 0.″38 wide radial slices) falls off symmetrically with respect to the minor axis outward from the location of the star. In the directions of the maximum extent of the scattered-light pattern (red and green "cuts" overlaid on the image inset), the surface brightness declines as $r^{-2.6\pm0.1}$ from 0.″7 to 5.″0. Along the southern minor axis, the surface brightness declines as $r^{-2.0}$ from 0.″7 to 1.″4 and as $r^{-5.0}$ from 1.″4 to 2.″6. The outer part of the scattering region shown in red in the image inset is detected with $> 3\ \sigma$ per pixel significance and corresponds to the outer blue contours in Figure 2. Beyond, additional scattered light is seen declining to levels of a few μmJy arcsec^{-2} at the sensitivity limits of the observation to r ~ 7 ″.